



# **Megavolt Accelerator Systems for Environmental Monitoring at ANSTO**

**Prof. David D. Cohen**

**The Centre for Accelerator Science (CAS)  
Australian Nuclear Science and Technology Organisation**

**January 2023**

**ISSN - 1030-7745**

**ISBN: 1 921268 36 0**



## Contents

1. Introduction .....	4
2. IONBEAM ANALYSIS .....	5
3. SOURCE APPORTIONMENT .....	7
4. HYSPLIT BACK TRAJECTORIES .....	10
5. ACCELERATOR MASS SPECTROMETRY .....	13
6. SUMMARY .....	17
7. ACKNOWLEDGEMENTS.....	18
8. REFERENCES .....	18

**Keywords:** Ion Beam Analysis, Accelerator Mass Spectrometry, PMF, air pollution, isotope dating.

### Abstract

The accelerator based ion beam techniques of ion beam analysis (IBA) and accelerator mass spectrometry (AMS) have been applied to environmental studies for many decades. IBA is particularly suited to fine particle air pollution studies where multi-elemental analysis of microgram samples is required. AMS, using  $^{14}\text{C}$  isotope, is a key tool for climate change studies and other isotopes like  $^{36}\text{Cl}$  and  $^{10}\text{Be}$  can be applied to ground water and soil erosion studies depending on the isotopic half-life and timescale being used.

Megavolt accelerator systems together with modern detector systems are capable of individual atom and photon counting and consequently are very sensitive detection systems. They are capable of precise and accurate measurements on very small sample sizes. The multi-element IBA technique of PIXE is capable of measuring some elements with ( $\mu\text{g/g}$ ) sensitivity on picogram (pg) samples. The AMS techniques used in  $^{14}\text{C}$  analysis have achieved dates out to 50,000 years on 10  $\mu\text{g}$  samples.

**Email:** [David.Cohen@ansto.gov.au](mailto:David.Cohen@ansto.gov.au)

---

## **MEGAVOLT ACCELERATOR SYSTEMS FOR ENVIRONMENTAL MONITORING AT ANSTO**

DAVID D. COHEN

Centre for Accelerator Science, Australian Nuclear Science and technology Organisation, Menai,  
NSW, Australia

### **1. INTRODUCTION**

Accelerator based ion beam analysis (IBA) and mass spectrometry (AMS) techniques have been applied successfully to environmental studies for many decades [1-4]. Megavolt accelerators are ideally suited for these studies. They are very sensitive, capable of individual atom or photon counting and they can analyse very small samples, picograms to microgram in just a few minutes of beam time [5-7].

In particular, IBA and AMS have been used to study climate change both current and past. It is accepted by the majority of scientists that climate change is here now [8]. 2021 was the sixth warmest year since 1880, eight of the top ten warmest years on our planet occurred in the last decade. Global temperatures have risen 0.85°C above the 1951-1980 average with a 1.1°C increase since the Industrial Revolution around 250 years ago. Greenhouse gases like carbon dioxide account for approximately +2.5W/m<sup>2</sup> of global warming [8]. <sup>14</sup>C AMS studies can date carbon dioxide levels in ice cores going back 50,000 years [2,4]. It can distinguish between modern and ancient carbon to better understand the past and present levels of this greenhouse gas.

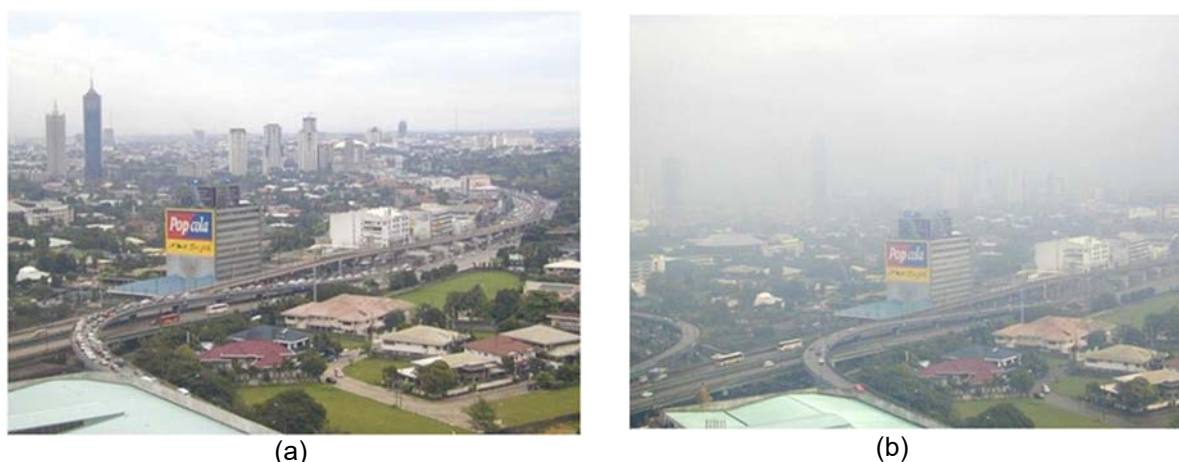
Fine particle pollution in the atmosphere from fossil fuel combustion like ammonium sulfate, secondary organics and black carbon have a total negative climate forcing of around -1.1W/m<sup>2</sup> reducing the impact of the greenhouse gases. Without fine particle pollution the current global temperature rise would be even higher than it currently is [8].

Fig. 1 shows fine particle pollution in Manila, Philippines on a clear and a polluted day. It demonstrates that fine particle pollution also affects visibility. Indeed, the eyes are a good detector of fine particle pollution.

Fine particle pollution is driven by the current trend globally to urbanisation [9-14]. The movement of large numbers of people from rural areas to the cities. Everyday more than 100,000 people globally move into cities. Since 2008, more than 50% of the world's population lives in cities. These cities become megacities with populations in excess of 10M people. Currently there are more than 37 megacities globally with eight out of the top ten megacities occurring in the Asia region. As cities get bigger more and more resources are needed to generate the power needed and the food required to feed and sustain them.

The IAEA has run a very successful fine particle pollution characterisation research program for decades across more than 15 countries in Asia from Pakistan in the west to the Philippines in east and Mongolia in the north to New Zealand and Australia in the south. This program has helped national

programs understand their air pollution issues in megacities and also identified long range pollution transport across international borders.



*FIG. 1 Aerial view of Manila, Philippines on (a) a clear day and (b) a fine particle polluted day showing the reduction in visibility produced by fine particle pollution.*

Fine particle pollution has recognised health effects [15]. Even annual fine particle pollution levels as low as  $10\mu\text{g}/\text{m}^3$  have health impacts, some megacities have annual average pollution levels over  $50\mu\text{g}/\text{m}^3$ . There appears to be no threshold limit for these health impacts. Fine particle pollution shortens life expectancy. It has been estimated that the average life expectancy of a person living in a major Asian megacity is reduced by between 5 to 6 years. In the State of NSW in Australia, with a population of only 6M and which has relatively clean air most days of the year, it is estimated that 420 a year die prematurely from fine particle air pollution. This is more than are killed on the roads by motor vehicles in NSW each year.

## **2. IONBEAM ANALYSIS**

The IBA techniques of Particle Induced X-ray Emission (PIXE), Particle Induced Gamma Ray Emission (PIGE), Rutherford Backscattering (RBS), Particle Elastic Scattering Analysis (PESA) most commonly used on these machines, all have several key properties in common. They can measure micrograms of sample with parts per million sensitivity non-destructively in just a few minutes of accelerator running time. Fine particles, collected on filters are such samples. For average fine particle air pollution levels of  $10\mu\text{g}/\text{m}^3$ ,  $30\text{ m}^3$  of air passed through a filter in 24 hours will contain only  $300\mu\text{g}$  of sample.

PIXE has been used since the mid 1970's to analysis filters obtained to characterise fine particle air pollution. Tens of thousands of such filters have been analysed to date across the globe in Europe, Africa, South America, Middle East and Asia by dozens of laboratories with megavolt accelerators. To date, these methods have been greatly refined.

All four IBA techniques of PIXE, PIGE, RBS and PESA can be run simultaneously to determine over 30 different elements from hydrogen to lead at concentrations from a  $\text{ng}/\text{m}^3$  to hundreds of  $\mu\text{g}/\text{m}^3$  of

air sampled. Typically, a few nanoamps of 3 MeV protons with beam diameters of several millimetres are used to irradiate each filter.

Fig.2 shows the 2MV STAR accelerator at ANSTO. The high energy beamline and end station in the central foreground, is the environment beam line used for IBA analysis of Teflon filters used to collect fine particle pollution.

A typical 25mm stretched Teflon filter is shown in Fig.3. This filter was loaded with fine particles collected by a PM2.5 fine particle cyclone system using a flow rate of 22l/min and collected over a 24 hour period from midnight to midnight.



*FIG.2. ANSTO 2MV STAR accelerator used in IBA studies with two high energy beamlines in the foreground.*



*FIG. 3. Exposed stretched Teflon filter, optimised for IBA analysis of fine particulate matter.*

The four IBA techniques described above produce four unique spectra, these spectra are shown in Fig. 4 for a typical stretched Teflon filter. Each spectrum was run for 3  $\mu\text{C}$  of 2.5 MeV protons. These x-ray PIXE spectra provides data on elements from Al to Pb. The x-ray energy is characteristic of the element present and the area under each characteristic peak is related to the concentration of that

element. In the PIXE spectra we see evidence of possible pollution sources associated with key elements. For example, Al, Si and Ti from wind blown soils, Cl from sea spray, K from biomass burning, Ca from cement production, metals from industry and Br and Pb from the use of leaded petrol in automobiles. In the PIGE gamma ray spectrum the photon energy is higher than for x-rays with peaks identifying elements such as F at 197 keV, Na at 440 keV. Again, the area under these gamma peaks is related to the elemental concentrations. The RBS spectrum is used to determine the low Z elements C, N and O [3,6]. The blue vertical lines show the front edge back scattered energies for these elements. The area from these front edge energies back to lower energies is used to estimate the total C, N and O concentrations. The PESA spectrum is used to measure the total H concentration. Hydrogen is the lightest element in the periodic table so its peak is to the left of all other element peaks in this spectrum. All these four spectra were analysed using the iBAT codes to obtain peak areas and elemental concentrations [16].

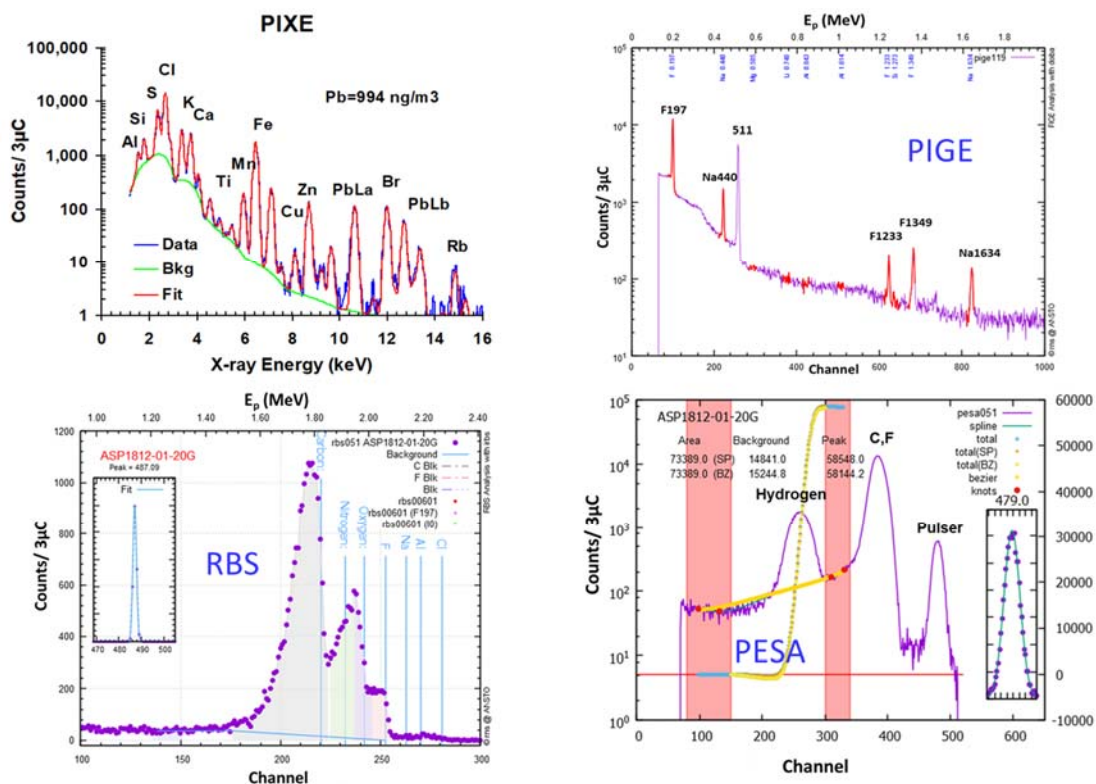


FIG. 4. PIXE, PIGE, RBS and PESA spectra for a typical exposed stretched Teflon filter.

For these spectra minimum detectable limits (MDL) for most elements range from 1 ng/m<sup>3</sup> to 10 ng/m<sup>3</sup> of air sampled through the filter. MDLs for the low atomic number elements using PIGE tend to be a bit higher at 50 ng/m<sup>3</sup> to 100 ng/m<sup>3</sup>.

### 3. SOURCE APPORTIONMENT

The elemental outputs from these methods can be used as input for statistical source apportionment methods such as Positive Matrix Factorisation (PMF) to generate elemental source fingerprints and to then determine the contribution of these fingerprints to the total measured mass of fine particles in the air [17]. PMF is a one step process that that takes the daily mass matrix  $M_{ij}$  and determines



a fingerprint matrix  $F_{kj}$  with a fingerprint contribution matrix  $G_{ik}$  by minimizing the error term  $E_{ij}$  in the equation,

$$M_{ij} = \sum_{k=1}^p F_{kj} * G_{ik} + E_{ij}$$

Depending on the number of daily measurements and the number of chemical species measured for each day the number of source fingerprints can range from 5 to 10 [18-20].

For example, Fig. 5 shows the PMF fingerprints obtained for 2,303 PM2.5 daily filters at an urban site in Sydney, Australia for the period from January 1998 to February 2022. Eight fingerprints, *Soil*, *Aged Sea Spray*, fresh *Sea Spray*, *Secondary Sulfate*, *Smoke* from biomass burning, two *Automobile* fingerprints and an *Industrial Nitrate* fingerprint were obtained. Each fingerprint is composed of 24 elements and chemical species from H to Pb with black carbon (BC) and ammonium nitrate (NO<sub>3</sub>) included. The average PM2.5 mass over this 24 year period was (8.1±5.2 µg/m<sup>3</sup>). That is the total mass of 8.1 µg/m<sup>3</sup> was divided into eight different and statistically significant source fingerprints. The 24 year average percentage contribution to this mass for the eight sources were 2.56%, 14.7%, 9.17%, 24.5%, 29.5%, 14.0%, 1.94% and 3.75% respectively and are shown on each of the eight plots in Fig. 5.

For each of these eight fingerprints the contributions of each element have been normalised to the element with the maximum impact for that fingerprint. This helps identify and put a name to each of these fingerprints. Note the y-axis *Source Fraction* is a four-decade log plot. The *Soil* fingerprint was driven by the elements Al, Si, Ca, Ti and Fe with the (Al/Si) ratio typical for clay aluminosilicates. The *Sea* fingerprint was driven by Na and Cl in the correct ratio for NaCl and with traces of Si, Ca and Br. The *Secondary Sulfate (2ndryS)* fingerprint was driven by H and S in the correct ratio for ammonium sulfate. The *Smoke* fingerprint was driven by H reflecting the organic component, K indicative of biomass burning, black carbon (BC) for the soot content and other trace elements such as Cl, Zn and Br typical of biomass burning.

Of the two automobile fingerprints *Auto2* represents vehicles using leaded petrol which was banned in January 2001 and so its 24 year average was quite low being essentially zero for 20 years of this study period. Nevertheless, the PMF technique was able to extract this out as a separate fingerprint. The technique was also able to provide information on chemistry that takes place in airborne aerosols as they age. The sampling site was 30 km from the coast and received significant sea breezes in the summer periods. During the transport of sea salts across major urban and semi-industrial regions to the sampling site chemical reactions between the NaCl based salts reacting with the secondary sulfates produced an *Aged Sea Salt (Seaaged)* fingerprint stripped of Cl and high in S. Demonstrating the production of a sodium sulfate aerosol. This demonstrates the power of the PMF statistical method in identifying sources and their contributions.



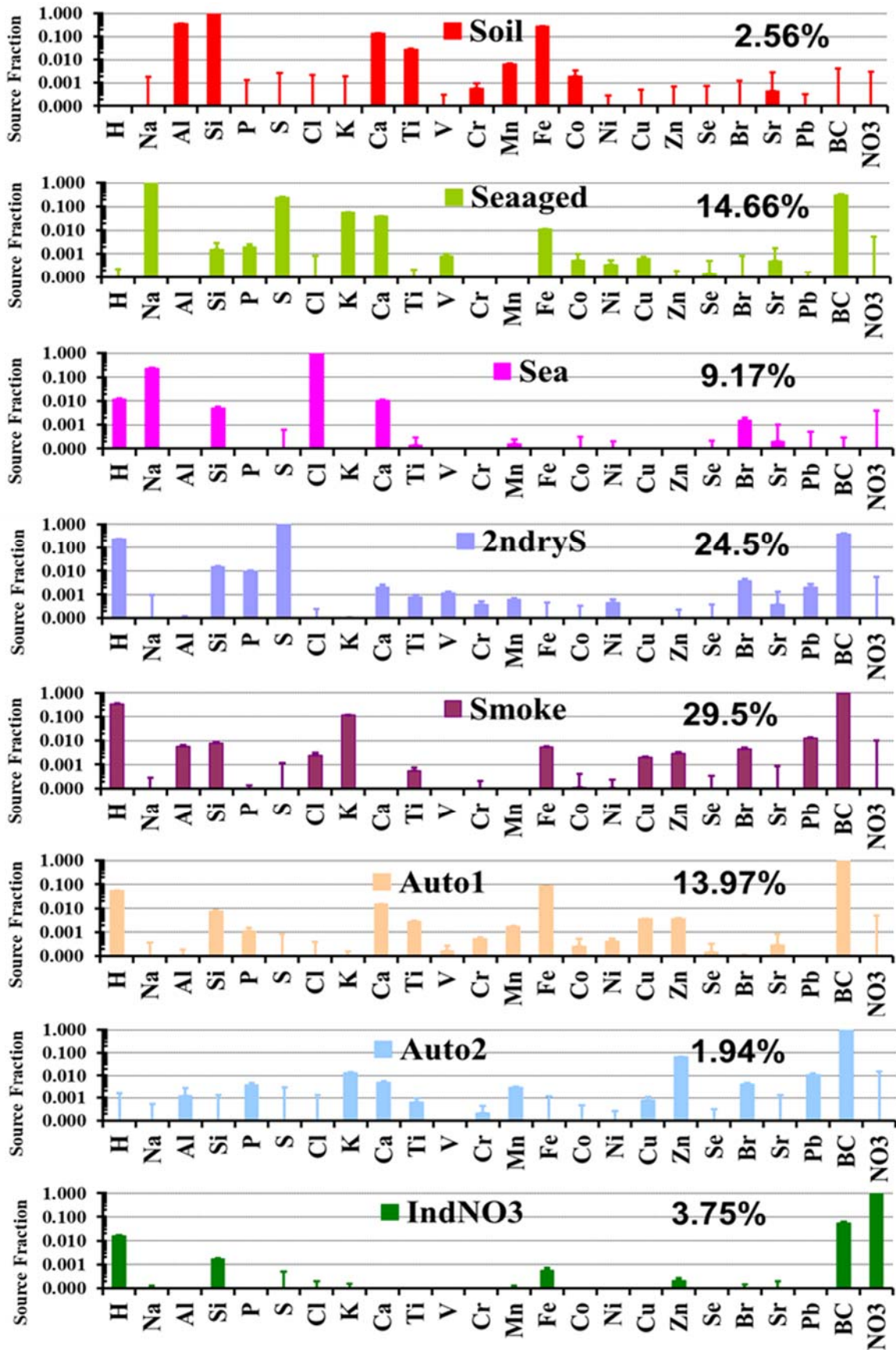


FIG. 5. PMF eight fingerprint fit to 24 years of PM<sub>2.5</sub> mass data at the Liverpool site in Sydney Australia.

The PMF technique also provides the daily contribution of each fingerprint to the total PM<sub>2.5</sub> mass. This is obtained from the  $G_{ik}$  matrix. Fig. 6 is a plot of the daily *Soil* fingerprint concentration shown in Fig. 5 from January 2001 to February 2022.

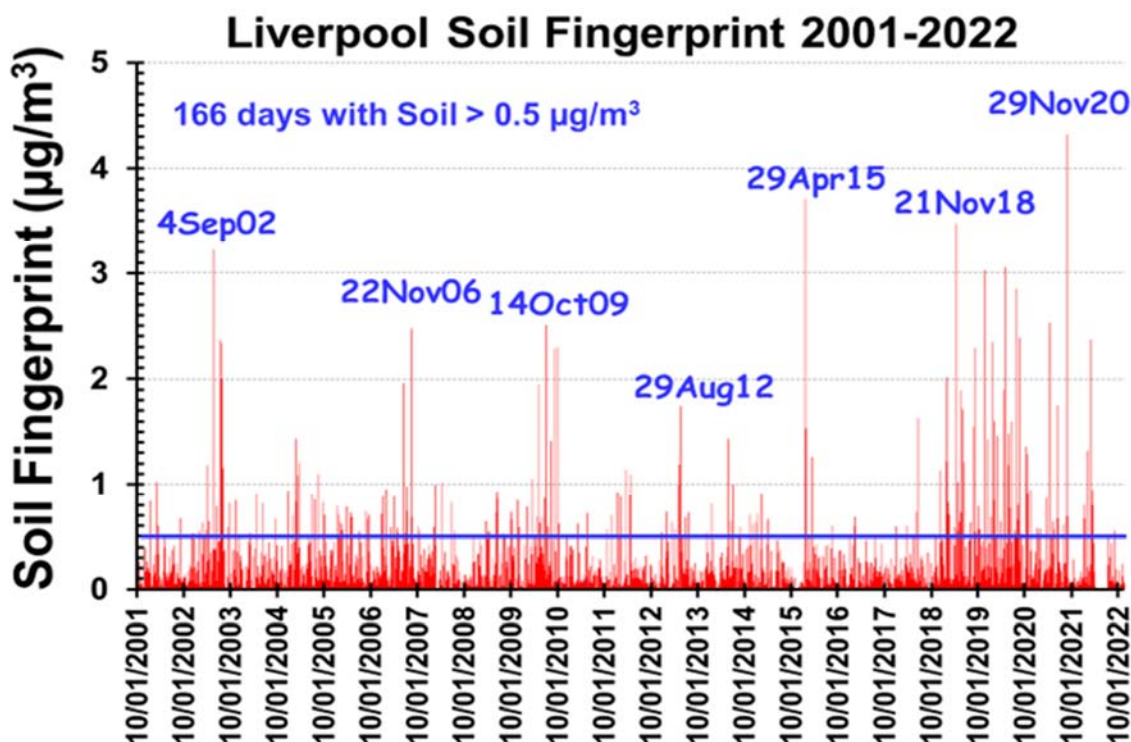


FIG. 6. A time series plot from January 2001 to February 2022 of the *Soil* fingerprint in Fig. 5.

At this Liverpool site in Sydney, Australia there were several possible soil sources, these included desert dust storms, soil from agricultural activities such as ploughing and retrained road dust produced by vehicular movements. Dust storms and agricultural soil can be transported over large distances whereas retrained road dust tends to be a more constant source and to be localised. Fig. 6 shows that there were 166 days with the *Soil* fingerprint concentrations above 0.5 µg/cm<sup>3</sup>. This upper-level soil concentration of 0.5 µg/m<sup>3</sup> was arbitrarily fixed but hopefully concentrations below this would include most retrained soil events. Some individual high *Soil* dates at the Liverpool site are labelled in Fig.6. There were clearly many more major *Soil* events between 2018 and 2021 with levels above 2 µg/m<sup>3</sup> than in previous years. The 166 daily soil events above 0.5 µg/cm<sup>3</sup> probably include most desert dust and agricultural soil events which are discussed further in the next section.

#### 4. HYSPLIT BACK TRAJECTORIES

The PMF source fingerprinting methods can be taken a step further with the application of hourly wind speed and direction data to pinpoint the location and long-range transport of these pollution sources often many hundreds of kilometres. The HYSPLIT codes contain hourly wind speed and direction data,

based on 1°x1° grids for anywhere on the globe and are freely available on the WEB [21-22]. In our current region of interest (Australia), a 1°x1° grid corresponds to approximately 100kmx100km area.

Australia is one of the driest continents on earth and has at least fourteen major deserts mainly across its central regions. Major desert dust storms, like the one shown in Fig. 7 are readily identified as impacting at sampling sites in the Sydney basin by not only the unusually high winds needed to transport them there but also the red dust associated with the transport of soils rich in iron oxides. A basic question is - what is the major *Soil* source transporting significant soils into the Sydney basin when you consider every hour of every day for several decades?



FIG. 7. Desert dust storm in Birdsville, Queensland, Australia. 27 January 2006

Using HYSPLIT data, the Liverpool site in Sydney and a height of 300m as a starting point for hourly seven day back trajectories for each of the 166 days with the *Soil* fingerprint concentrations above 0.5  $\mu\text{g}/\text{m}^3$  we can backtrack the source of the *Soil* on each of these days. Fig. 8 is plot of the desert regions across Australia. It contains 14 boxes representing the 14 desert regions and a fifteenth box representing the agricultural region of the Riverina in state of NSW. Twenty four one hourly back trajectories for 4 September 2002 and 8 May 2019 are shown as typical examples of daily back trajectories. The 8 May 2019 back trajectory shows several of the hourly seven day back trajectories on that day passing through several of the desert boxes including box 8 (The Great Victoria Desert West) over 2,800 km west of the Liverpool site. The 4 September 2002 back trajectory was further south of the 8 May 2002 back trajectory. It spent much of its seven days over the ocean, mainly passing through box 15, the Riverina, an agricultural region in NSW in the first few days of its 7 day back trajectory.

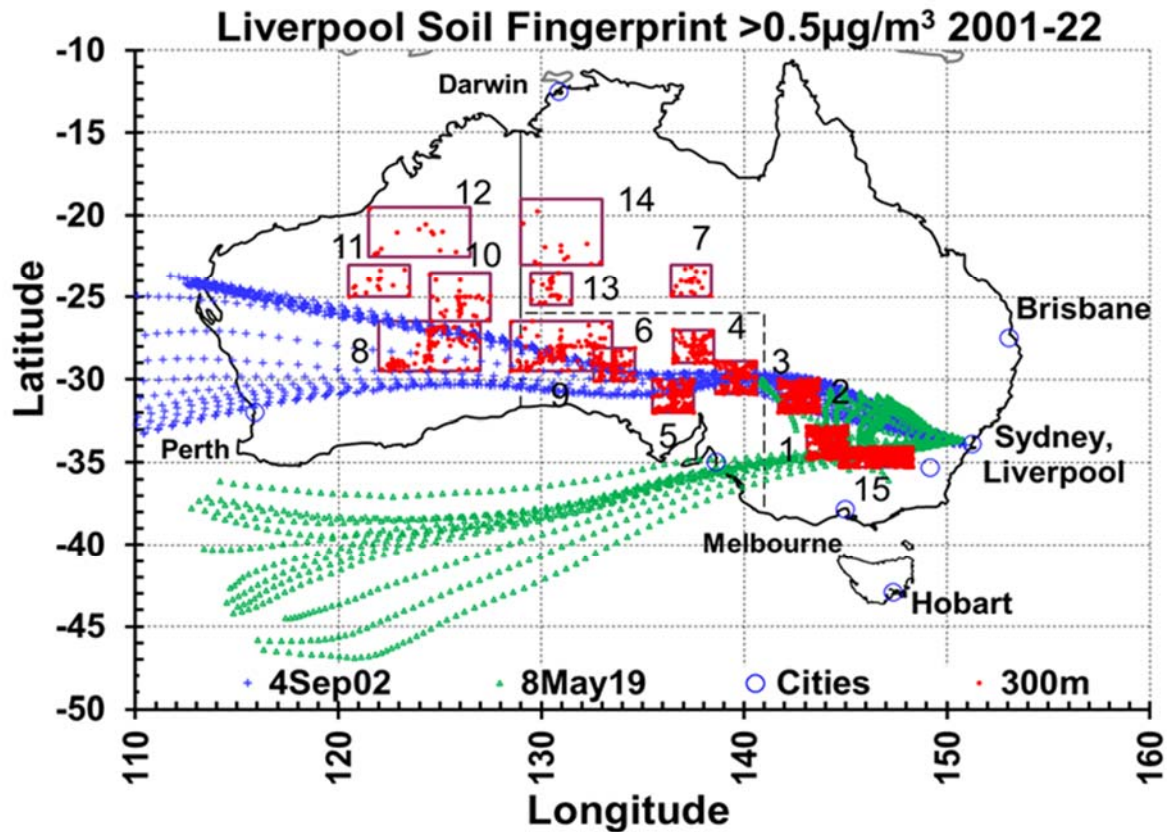


FIG. 8. Map of desert regions represented by boxes 1-14 and one major agricultural region box 15. The blue (+) signs and the green (..) represent 24 hourly back trajectories for the 4 September 2002 and 8 May 2019 respectively at starting height of 300m at the Liverpool site.

We have continued this process for every hour of every day for all of the 166 days with a high *Soil* fingerprint during the study period from January 2001 to February 2022. Every time a 7 day hourly back trajectory crossed any one of the 15 boxes a dot was placed in that box. The number of dots in each box then presented the number of times that desert region could have contributed to the *Soil* measured at the Liverpool site in the Sydney basin during the twenty two years from January 2001 to February 2022. Table 1 summarises the percent of back trajectories crossing each of these box regions.

TABLE 1. A SUMMARY OF THE PERCENT OF BACK TRAJECTORIES CROSSING EACH OF THE FIFTEEN BOX REGIONS IN FIG. 8.

300m Desert	Trajectories (%)	Desert	Trajectories (%)
15 Riverina	41.2	6 Lake Eyre North	2.1
1 Lake Mungo	25.6	10 Gibson	0.7
2 Lake Windaunka	11.8	7 Simpson Desert	0.5
4 Olympic Dam	5.2	13 Great Sandy East	0.5
3 East Flinders	4.6	11 Little Sandy	0.4



9 Great Vic E	2.4	12 Great Sandy West	0.3
8 Great Vic West	2.2	14 Tanami	0.3
5 Emu Fields Salt	2.2		

The maximum percent of back trajectories (41.2%) crossed box 15, the Riverina agricultural region followed by the Lake Mungo desert region with 25.6% of all trajectories. *Soil* from these two regions was responsible for more than two thirds of the *Soil* entering the Sydney basin during the twenty two years from January 2001 to February 2022. The remaining thirteen desert regions only contributed about one third of the time to *Soil* levels in Sydney above  $0.5 \mu\text{g}/\text{m}^3$ . The Riverina and Lake Mungo regions are between 500 and 600 km WSW from the Liverpool site in the Sydney basin so soil from these regions represented long range transport of PM2.5 particles.

## 5. ACCELERATOR MASS SPECTROMETRY

Accelerator mass spectrometry (AMS) is a dating technique base on the half-life of isotopes. Megavolt accelerators can accelerate almost any isotope in the periodic table. They have the potential to determine isotopic ratios down to 1 part in  $10^{15}$  in microgram samples with a precision approaching 0.5%. It is a dating technique capable of measuring dates out to around ten half-lives of the isotope being considered [2].

The method is based on the selected isotopes rigidity when passing through the entire accelerator system from the ion source to the end station's detector system [2,4]. The rigidity of an ion of mass  $M(\text{amu})$  with charge  $q$  and energy  $E(\text{MeV})$  is defined as  $(ME/q^2)$ . Machine energies and ion charge states, magnetic fields and electrostatic fields along the ions path to the detection system are specifically selected to only pass the desired isotope of interest. For example, chlorine has many isotopes including  $^{35}\text{Cl}$ ,  $^{36}\text{Cl}$  and  $^{37}\text{Cl}$ .  $^{35}\text{Cl}$  (76%) and  $^{37}\text{Cl}$  (24%) are naturally occurring and stable whereas  $^{36}\text{Cl}$  is radioactive and the isotopic ratio ( $^{36}\text{Cl}/\text{Cl}$ ) in the environment is typically only 1 part in  $7 \times 10^{13}$ . In order to separate isotopes whose masses are close together, like  $^{35}\text{Cl}$  and  $^{36}\text{Cl}$ , traditionally large tandem accelerators with voltages in the 5-10 MV range together with their associated large magnet systems have been used [4]. Fig. 9 shows the 10 MV ANATARES FN Tandem accelerator at ANSTO in Sydney, Australia used for AMS studies. This accelerator is capable of detecting heavy actinide isotopes like  $^{235,236}\text{U}$  and  $^{242,244}\text{Pu}$ . The low energy injection magnet and the high energy analysing magnet have  $(ME/q^2)$  of 20 and 72 respectively. Most of its magnet systems are capable of producing magnetic fields in excess of 1 Tesla and with ion charge states in excess of  $q = +10$  for heavy ions, energies above 100 MeV are possible.



(a)



(b)



(c)

FIG. 9. The 10MV ANTARES accelerator at ANSTO in Sydney, Australia (a) AMS ion source, (b) 10 MV tank and terminal and (c) the actinide AMS beamline and end station.

Modern ion sources have the ability to mount multiple cathodes on a wheel. For AMS each of these cathodes contains the isotopes of the atoms to be measured. Samples sizes as small as 10 $\mu$ g of carbon have been used for  $^{14}\text{C}$  dating analyses [2]. Fig. 10 shows typical cathodes used in cathode wheels which are mounted in the accelerator ion source. For sputter ion sources on Tandem accelerators these cathodes are typically bombarded with a cesium beam in the ion source to produce negative ions of the isotopes required. These negative isotopes are then accelerated by the positive terminal voltage in the tank before being stripped by gas or foil stripper to produce positive ions which are then accelerated to the end station and detection system.



FIG. 10. Typical cathode systems used in the accelerator ion source for AMS studies, left is a cathode and right are cathodes in an ion source cathode wheel.

Common isotopes used for environmental studies include  $^{14}\text{C}$  (5,730 years),  $^{36}\text{Cl}$  (301k years) and  $^{10}\text{Be}$  (1.386M years). Fig. 11 shows these three isotopes together span possible dates from the present



to 14M years and have applications for carbon dating in climate change studies,  $^{10}\text{Be}$  for soil erosion and formation and  $^{36}\text{Cl}$  for ground water studies.  $^{14}\text{C}$  is produced in the earth's atmosphere by thermal neutrons interacting with nitrogen.  $^{36}\text{Cl}$  by spallation of  $^{39}\text{K}$  and  $^{40}\text{Ca}$  and neutron reactions with the stable  $^{35}\text{Cl}$  isotope.  $^{10}\text{Be}$  is a long lived isotope produced by cosmic ray interactions with  $^{14}\text{N}$  and  $^{16}\text{O}$  and the spallation of  $^{16}\text{O}$ ,  $^{27}\text{Al}$ ,  $^{28}\text{Si}$  and  $^{56}\text{Fe}$  in rocks in the earth's surface.

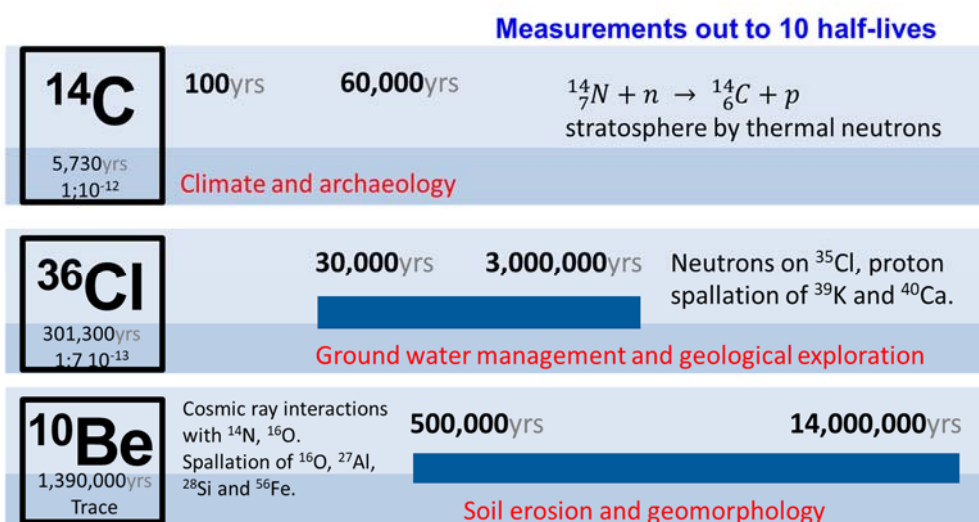


FIG. 11. Half-lives of three common AMS isotopes used in environment studies. They span a time frame from the present to 14M years ago.

Fig. 12(a) shows an ice core being extracted from the Antarctic ice shelf and Fig. 12(b) shows a typical section of ice (firn) containing historical gas bubbles. Firn is an intermediate stage in an ice core between the upper level snow and the fully compacted ice deeper down, Firn typically occurs between 40m and 120m deep, lower firn permanently traps the atmospheric gases and is therefore useful as a historical record of past atmospheric condition. This technique of extracting gases particularly, carbon dioxide and methane, can provide valuable information on atmospheric composition going back over 800,000 years [23-26].

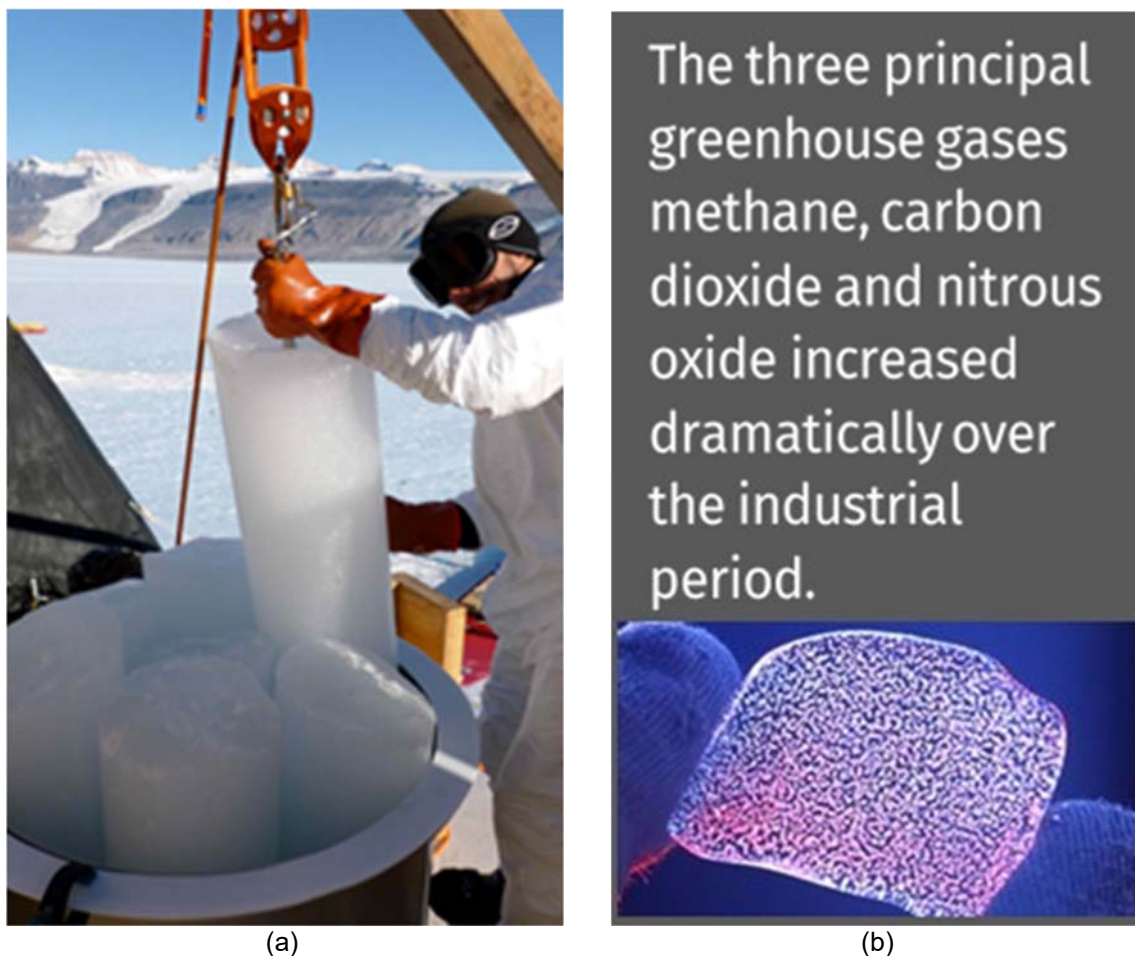


FIG. 12. (a) Extracting ice cores in Antarctica and (b) gases trapped in firn ice.

## 6. SUMMARY

IBA methods associated with megavolt accelerator systems are ideally suited to study fine particle pollution. The ability to analysis hundreds of samples very quickly with sensitivities of the order of 1-10 ng/m<sup>3</sup> means that powerful statistical source apportionment techniques like positive matrix factorisation can be applied to determine source fingerprints and their contributions to the total measured fine mass. Furthermore, by applying wind speed back trajectory methods, such as embedded in the HYSPLIT codes available generally on the WEB, the origins of these source fingerprints can be located. These combined methods demonstrate the ability of fine particulate pollution to be transported long distances across state and country borders and even across the globe.

Accelerator -based AMS dating techniques allow environmental samples to be dated with dates ranging from the present to millions of years old. If the isotope, of any given atom of interest, is appropriately selected megavolt accelerator systems can be used to determine isotopic ratios to better than 1 part in 10<sup>15</sup> with precision in some cases exceeding 0.5%.

Megavolt accelerator systems together with modern detector systems are capable of individual atom and photon counting and consequently are very sensitive detection systems. They are capable of precise and accurate measurements on very small sample sizes. The multi-element IBA technique of

PIXE is capable of measuring some elements with ( $\mu\text{g/g}$ ) sensitivity on picogram ( $\text{pg}$ ) samples. The AMS techniques used in  $^{14}\text{C}$  analysis have achieved dates out to 50,000 years on 10  $\mu\text{g}$  samples.

## 7. ACKNOWLEDGEMENTS

I would like to acknowledge the support of the staff of Centre for Accelerator Science at ANSTO and the National Collaborative Research Infrastructure Scheme (NCRIS) whose technical and financial support helped provide some of the data used in this document.

## 8. REFERENCES

- [1] R. BIRD AND J. WILLIAMS, Ion Beams for Materials Analysis, November 1989, ISBN 9780080916897.
- [2] TUNIZ, C., et al., Accelerator mass spectrometry: ultrasensitive analysis of global science. 1998, United States: CRC Press.
- [3] COHEN D.D., 1998: Characterisation of Atmospheric Fine Particle Using IBA Techniques. Nuclear Instruments and Methods in Physics Research B, 136B, 14-22.
- [4] PASTUOVIC, ZELJKO BUTTON, DAVID COHEN, DAVID FINK, DAVID GARTON, DAVID HOTCHKIS, MICHAEL IONESCU, MIHAIL LONG, SHANE LEVCHENKO. VLAD MANN, MICHAEL SIEGELE, RAINER SMITH, ANDREW WILCKEN. KLAUS SIRIUS – A new 6MV accelerator system for IBA and AMS at ANSTO. Nucl. Instr. and Methods in Phys. Res., B371 (2016)142-147.
- [5] COHEN D.D., STELCER E., GARTON D., 2002: Ion beam methods to determine trace heavy metals concentrations and sources in urban airsheds. Nuclear Instruments and Methods in Physics Research B190, 466-470.
- [6] COHEN D.D, GARTON D., STELCER E., HAWES O., 2004: Accelerator based studies of atmospheric pollution processes. Radiation Physics and Chemistry 71, 758-567.
- [7] COHEN D.D., STELCER E., GARTON D., CRAWFORD J., 2011: Fine Particle Characterisation, Source Apportionment and Long Range Dust Transport into the Sydney Basin: A long term study between 1998 and 2009. Atmospheric Pollution Research 2, 182-189.
- [8] INTERGOVERNMENTAL PANEL FOR CLIMATE CHANGE (IPCC) report, *Summary for Policymakers*, April 2022, [https://www.ipcc.ch/site/assets/uploads/sites/2/2022/06/SPM\\_version\\_report\\_LR.pdf](https://www.ipcc.ch/site/assets/uploads/sites/2/2022/06/SPM_version_report_LR.pdf)
- [9] BAYER, P., KEOHANE, N., TIMMINS, C., 2009. Migration and hedonic valuation: The case of air quality. Journal of Environmental Economics and Management 58, 1-14.
- [10] GUANGSHIAXILU, HONGXIAZHANG, HAOTIANZHENG, ZHONGHUA ZHANG, SHICHENAJIAXING, SHUXIAOWANG. Air pollutant emissions induced by rural-to-urban migration during China's urbanization (2005–2015) Environmental Science and Ecotechnology 10, (2022), 100166.
- [11] ZHAO, Y., 1999. Leaving the countryside: rural-to-urban migration decisions in China. The American Economic Review 89, 281-286.
- [12] THIEDE, B., GRAY, C., MUELLER, V., 2016. Climate variability and inter-provincial migration in South America, 1970–2011. Global Environmental Change 41, 228-240.
- [13] QIN, Y., ZHU, H., 2018. Run away? Air pollution and emigration interests in China. Journal of Population Economics 31, 235-266.
- [14] RAFIQ, S., NIELSEN, I., SMYTH, R., 2017. Effect of internal migration on the environment in China. Energy Economics 64, 31-44.
- [15] POPE, C.A., DOCKERY, D.W., 2006. Health effects of fine particulate air pollution: Lines that connect. Journal of the Air & Waste Management Association 56, 709-742.
- [16] SIEGELE, RAINER, COHEN, DAVID D., iBAT: A new ion beam batch analysis tool for thin samples. Nucl. Instrum. and Methods B493 (2021) 35-43.

- 
- [17] PAATERO, P., TAPPER, U., 1994: Positive matrix factorisation: a non-negative factor model with optimal utilization of error estimates of data values. *Environmetrics* 5, 111-126.
- [18] COHEN D.D., CRAWFORD J., STELCER E., ATANACIO A., 2012: Application of positive matrix factorisation, multi-linear engine and back trajectory techniques to the quantification of coal fired power station pollution in metropolitan Sydney. *Atmospheric Environment*, 61, 204-211.
- [19] COHEN, DAVID D. ATANACIO, ARMAND CRAWFORD, JAGODA SIEGELE RAINER. Ion beam techniques for source fingerprinting fine particle air pollution in major Asian-Pacific cities. *Nucl. Instrum. and Methods B477* (2020) 122-132.
- [20] COHEN D.D., STELCER E., ATANACIO A., CRAWFORD J., 2014: The application of IBA techniques to air pollution source fingerprinting and source apportionment. *Nucl. Instrum. and Methods*, B318, 113-118, doi:<http://dx.doi.org/10.1016/j.nimb.2013.05.093>.
- [21] DRAXLER R.R., 1991. The accuracy of trajectories during ANATEX calculated using dynamic model analysis versus rawinsonde observations. *Journal of Applied Meteorology* 30, 1466-1467.
- [22] DRAXLER R. R., ROLPH G.D, 2003. HYSPLIT (HYbrid Single-Particle Lagrangian Integrated Trajectory) Model access via NOAA ARL READY Website (<http://www.arl.noaa.gov/ready/hysplit4.html>). NOAA Air Resources Laboratory, Silver Spring, MD.
- [23] DYONISIUS, M.N., et al., Old carbon reservoirs were not important in the deglacial methane budget. *Science*, 2020. 367(6480): p. 907-910.
- [24] HMIEL, B., et al., Preindustrial  $^{14}\text{C}$  indicates greater anthropogenic fossil  $\text{CH}_4$  emissions. *Nature*, 2020. 578(7795): p. 409-412.
- [25] BUIZERT, C. Ice Core Methods | studies of firn air. *Encyclopedia of Quaternary Science* (Second Edition) 2013, Pages 361-372.
- [26] BROOK, E.J. Ice Core Methods | Overview. . *Encyclopedia of Quaternary Science* (Second Edition) 2013, Pages 277-287.

